International Journal of Applied Electromagnetics and Mechanics 15 (2001/2002) 377–382
IOS Press


# A Study of planar inductor

T. Naruta*, H. Endo, S. Hayano and Y. Saito
*College of Engineering, Hosei University, 3-7-2 Kajinocho, Koganei, Tokyo 185-8584, Japan*

**Abstract.** In order to design an optimal planar inductor, this paper carries out several axisymmetrical magnetic field simulations fully taking the magnetic hysteretic properties of ferromagnetic core materials as well as open boundary condition into account. Finite element method is applied to evaluating the magnetic fields, reactive and dissipative energies in a planar inductor. Because of the nature of magnetic fields, it is essentially taken into account the open boundary effects to evaluate the exact characteristics of planar inductor. Since the finite elements is one of the methodologies to solving for the partial differential equations, and then it has been difficult to take the open boundary effects into account. However, this paper removes this difficulty by employing the strategic dual image (SDI, in short) method [1,2]. Another difficulty is caused by the hysteretic magnetization characteristics of magnetic core materials. Applying the Chua type magnetization model to represent the hysteretic property also removes this difficulty. As a result, it is revealed that the frequency characteristic of core magnetic materials as well as shape dominate major characteristics of the magnetic fields, reactive and dissipative energies in the inductors.

## 1. Introduction

With the developments of modern hand held electronic devices, it is essentially required to develop the planar shape of magnetic elements, such as the electric transformer and inductor. Modern portable electronics are composed of the two major counterparts: one is the electronics processing the electronic signals, and the other is the electrical power supplier, which enables the electronic operations. The former can be constructed in the lightweight and thin shape by means of the printed circuits embodied with the large scale integrated circuits (LSI in short). However, since the latter supplies the electrical power to the signal processing elements, then it is difficult to construct in the lightweight and thin shape by means of the conventional design strategy.

To develop the thin shape magnetic power elements, in the present paper, we carry out the numerical simulations of a thin shape planar inductor by means of the finite elements fully taking into account the open boundary condition as well as hysteretic magnetization properties of core materials.

At first, we introduce the strategic dual image (SDI in short) method in order to take the open boundary condition into account [1,2].

Secondly, we carry out the intensive numerical simulations in order to searching for the optimal magnetic material under the realizable conditions. This means that our simulation takes into the hysteretic magnetization characteristic of core materials by means of the Chua type magnetization model [3,4].

As a result, it is revealed that the frequency characteristic of core magnetic materials as well as shape dominate major characteristics of the magnetic fields, reactive and dissipative energies in the inductors.

*Corresponding author: Tomokazu Naruta, College of Engineering, Hosei University, 3-7-2 Kajinocho, Koganei, Tokyo, Japan. Tel.: +81 423 87 6220; Fax: +81 423 87 6220; E-mail: naruta@ysaitoh.k.hosei.ac.jp.

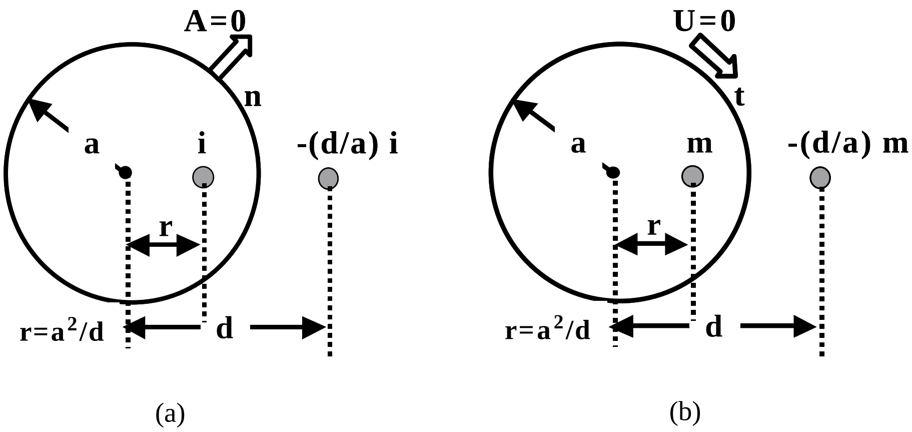


Fig. 1. (a)The rotational field source image $-(d/a)i$. The zero $\mathbf{A} = 0$ or symmetrical $\partial\mathbf{U}/\partial n = 0$ boundary condition is established at the circular/spherical surface. (b)The divergent field source image $-(d/a)m$. The zero $\mathbf{U} = 0$ or symmetrical $\partial\mathbf{A}/\partial n = 0$ boundary condition is established at the circular/spherical surface. Strategic 2D/3D dual images.

## 2. Strategic dual image method

At first, let us consider one of the currents $i$ in the problem region. When an image current – $(d/a)i$ is imposed at the position shown in Fig. 1(a), the normal component of magnetic flux density $\mathbf{B}$ becomes zero at the circular/spherical hypothetical boundary. This means that the vector potential $\mathbf{A}$ is zero at the hypothetical boundary when the magnetic field is represented in terms of $\mathbf{A}$. Moreover, this zero boundary condition $\mathbf{A} = 0$ corresponds to the symmetrical boundary condition $\partial\mathbf{U}/\partial n = 0$ when the magnetic field is represented in terms of scalar potential $\mathbf{U}$. The magnitude of image – $(d/a)i$ depends on the position of field source current i in the hypothetical boundary so that the following condition must be satisfied to reduce the zero net images,

$$a\sum_{p=1}^{q}(i_p/r_p) = 0, \tag{1}$$

where $a$ is radius of the circle/sphere; $r_p(= a^2/d_p)$ is the distance from the center of circle/sphere to the current $i_p$; and $q$ is the number of current sources. Equation (1) means that the net currents in the problem region must be zero, and the vector potential $\mathbf{A}$ becomes zero at the center of circular/spherical hypothetical boundary.

Secondly, let us consider one of the magnetic charges $m$ in the problem region instead of currents $i$. When an image $-(d/a)m$ is imposed at the position shown in Fig. 1(b), the tangential component of the field intensity $\mathbf{H}$ becomes zero at the hypothetical boundary. This means that the scalar potential $\mathbf{U}$ is zero at the hypothetical boundary when the magnetic field is represented in terms of $\mathbf{U}$. Moreover, this zero boundary condition $\mathbf{U} = 0$ corresponds to the symmetrical boundary condition $\partial\mathbf{A}/\partial n = 0$ when the magnetic field is represented in terms of the vector potential $\mathbf{A}$. Thus, a combination of the zero and symmetrical boundary solutions leads to an exact open boundary solution even if the finite elements.

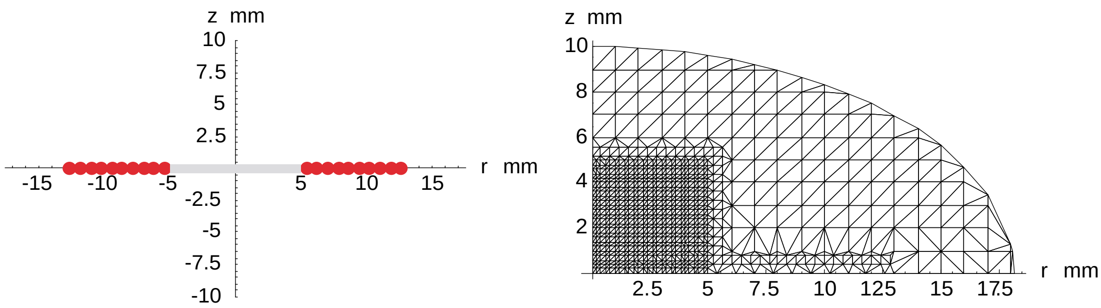


Fig. 2. Schematic diagram of a planar inductor and mesh system for FEM analysis.

## 3. Modelling of the magnetization characteristics

### 3.1. Chua type model

Chua type magnetization model, based on magnetic domain theory, is capable of representing the magnetization characteristics of ferromagnetic materials with sufficient accuracy. In this model given by Eq. (2), the magnetic field intensity $H$ is expressed as function of the magnetic flux density $\mathbf{B}$, the time derivative of magnetic field intensity $\mathrm{d}H/\mathrm{d}t$ and magnetic flux density $dB/dt$. It contains three parameters which are the permeability $\mu$, reversible permeability $\mu_r$ and hysteresis coefficient $s$.

$$H = \frac{1}{\mu}B + \frac{1}{s}\left(\frac{\mathrm{d}B}{\mathrm{d}t} - \mu_r\frac{\mathrm{d}H}{\mathrm{d}t}\right). \tag{2}$$

### 3.2. Complex permeability

At the high frequencies, the peak magnetic flux density in core is sufficiently small, so that it is possible to assume the sinusoidal time varying magnetic flux density $\mathbf{B}$ and magnetic field intensity $\mathbf{H}$. Therefore, the parameters $s$, $\mu$ and $\mu_r$ are assumed to be constants. According to the complex notation, the time derivation operator $d/dt$ can be replaced by $j\omega$, where $j$ and $\omega$ denote an imaginary number ($j = \sqrt{-1}$) and an angular frequency, respectively. In this way, Eq. (2) becomes a linear system. Thus, a complex permeability $\mu(\omega)$ given by Eq. (3) can be derived. This gives the hysteresis loops drawing an elliptical locus in shape.

$$\mu(\omega) = \frac{B}{H} = \frac{\mu(s^2 + \omega^2\mu\mu_r)}{s^2 + \omega^2\mu^2} - j\frac{\mu\omega s(\mu - \mu_r)}{s^2 + \omega^2\mu^2}. \tag{3}$$

## 4. Design of planar inductor

### 4.1. Model of planar inductor

To realize a high cost performance planar inductor, the inductor having the simplest shapes is examined in this paper. Figure 2 shows a schematic diagram of the planar inductor. The radii of coil and ferrite cores, and number of turns of exciting coil are 0.4 mm, 5.0 mm and 10turn, respectively. Also the thicknesses of ferrite cores are assumed to 0.8, 1.2, 1.6, 1.8, 5.0, and 10.0 mm

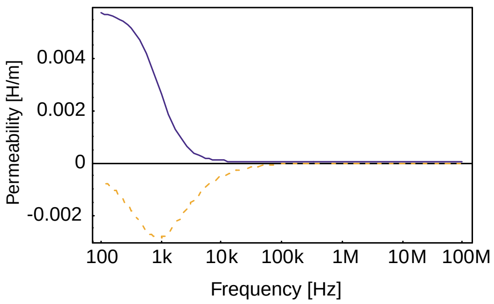


(a) H5c2 (TDK),

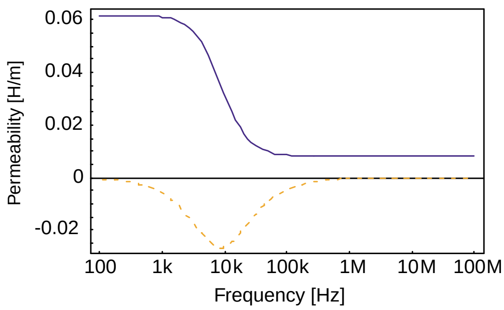


(b) H5A (TDK)

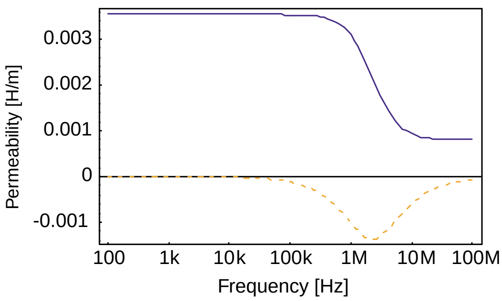


(c) 3S1 (Phillips)

Fig. 3. Frequency characteristics of the complex permeabilities (solid line : Real part, broken line : Imaginary part).

Table 1
Various parameters of the Chua type magnetization model

| Mn-Zn ferrite | $\mu$ [H/m] | $\mu_r$ [H/m] | $s$ $[\omega/\mathrm{m}]$ |
|---|---|---|---|
| H5c2 TDK Components | $5.78 \times 10^{-3}$ | $4.47 \times 10^{-5}$ | $3.0 \times 10$ |
| H5A TDK Components | $6.19 \times 10^{-2}$ | $8.17 \times 10^{-3}$ | $3.4 \times 10^{2}$ |
| 3S1 Phillips Components | $8.00 \times 10^{-3}$ | $0.80 \times 10^{-3}$ | $5.0 \times 10^{4}$ |

### *4.2. Frequency characteristics of the ferrite core*

We have selected the three typical types of ferrite cores for high frequency use, i.e., Mn-Zn type ferrites: H5c2 (TDK), H5A(TDK) and 3S1(Phillips). As is well known, the Mn-Zn type ferrite has the high permeability and high magnetic flux density even if high frequency use. Primary, Mn-Zn type ferrite has developed in order to reduce the eddy current loss by setting the low conductivity (0. [S/m]).As shown in Fig. 3, the Chua type model, whose parameters are listed in Table 1, represents the frequency characteristics of the ferrite cores.

## 5. Analysis of magnetic field distribution

We have assumed that the operating frequency of the planar inductor ranges from 100 [Hz] to 100 [MHz] in the simulations.

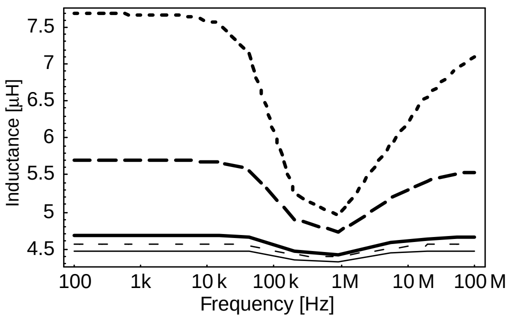


(a) Real part (H5c2)

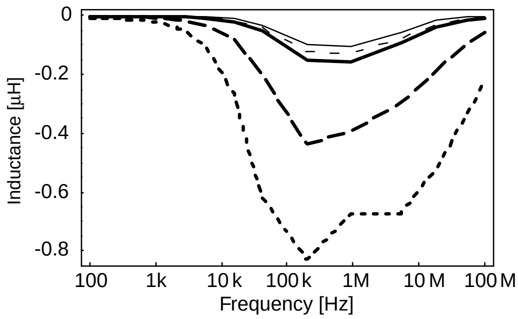


(b) Imaginary part (H5c2)

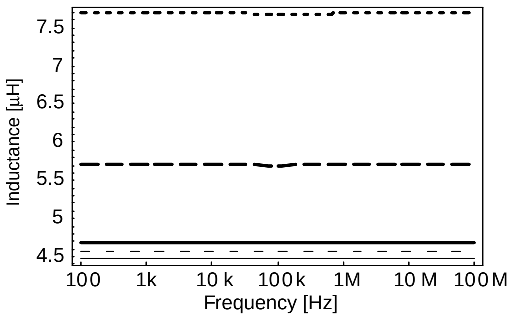


(c) Real part (H5A)

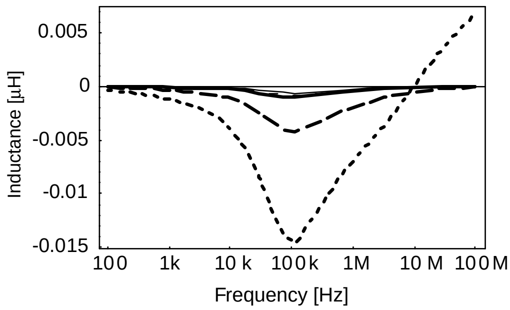


(d) Imaginary part (H5A)

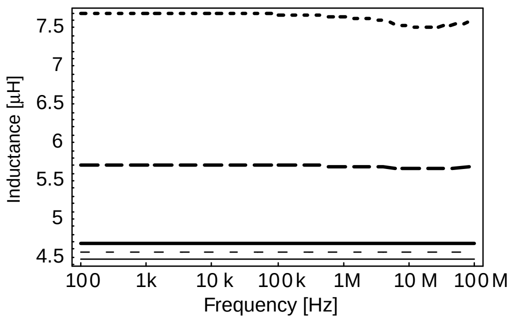


(e) Real part (3S1)

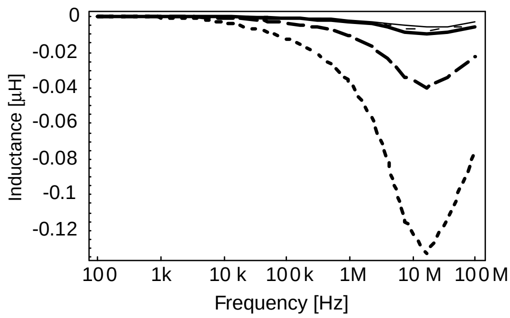


(g) Imaginary part (3S1)

The thickness of ferrite cores

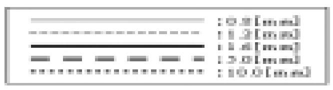

Fig. 4. The thickness of ferrite cores Frequency characteristics of planar inductor.

To evaluate the frequency characteristics of planar inductor, we computed the inductance. The inductance is generally classified into two parts. One is a real part, which corresponds to a reactive energy storing in the planar inductor. The other is an imaginary part, which corresponds to an energy loss in the planar inductor. Figure 4 shows the frequency characteristic of inductance.

Thus, it is clarified that the frequency characteristics of planar inductor become better than these of complex permeability shown in Fig. 3 This means that the demagnetization factor of planar inductors improves the frequency characteristics of the core materials, even though the inductance becomes smaller than those of the inductors having closed magnetic flux path.

## 6. Conclusions

To develop the thin and simplest shape inductor, we have carried out the numerical simulation of the thin shape planar inductor by means of the finite elements fully taking into account the open boundary condition as well as hysteretic magnetization property of core materials. The Chua type magnetization model has been employed in order to take the hysteretic property of magnetic materials into account. Also, the strategic dual image method has been applied to obtaining the open boundary finite elements solutions.

As a result, it has been clarified that the demagnetization factor of planar inductors improves the frequency characteristics of the core materials, even though the inductance becomes smaller than those of the inductors having closed magnetic flux path.

## References

[1] Y. Saito, Y. Nakazawa and S. Hayano, Faster open boundary magnetic field computation using the strategic dual image and Voronoi-Delaunay transformation methods, *Journal of Applied Physics* **67**(9) (1990).
[2] Y. Saito, K. Takahashi and S. Hayano, Finite element solution of unbounded magnetic field problem containing ferromagnetic materials, *IEEE Transaction on Magnetics* **MAG-24**(6) (1988).
[3] S. Hayano, I. Marinova and Y. Saito, New complex permeability measurement device for thin magnetic films, *Journal of Applied Physics* **75** (1994).
[4] S. Hayano, Y. Saito and Y. Sakaki, A magnetization model for computational magnetodynamics, *Journal of Applied Physics* **29** (1991).
[5] T. Naruta, S. Hayano and Y. Saito, 000 Wavelet Analysis of Optimization Problems – Designing of a flat shape magnetic sensor, *Journal of the Visualization Society of Japan* **20**(1) (2000), 336.
[6] K. Ohta, *Introduction to magnetic engineering I*, Kyoritsu shuppan, in Japanese, Tokyo, 1984.